Technical Communication

In situ corrosion studies on the Duart Point wreck, 1994

Ian Donald MacLeod
Department of Materials Conservation, Western Australian Museum, Cliff Street, Fremantle, Western Australia 6160

Introduction

The measurement of electrochemical parameters such as the surface pH and the corrosion potential, $E_{corr.}$, of degrading metal objects on wreck-sites has developed significantly from the early work on the *Rapid* (1811) in 1979 (MacLeod, 1981). The routine recording of on-site measurements has been an invaluable tool in understanding the corrosion mechanisms and the modes of deterioration of materials on marine archaeological sites. Analysis of the corrosion matrices and the *in situ* corrosion parameters can provide the archaeologist with a unique insight into what has occurred over the period of an object's deposition. From a knowledge of the present corrosion environment and from measurements of the accumulated effects of centuries of degradation there now exists a rational and non-destructive form of assessing the archaeological potential of metal objects on a wreck-site.

After an initially rapid rate of deterioration in the first few years of immersion most iron artefacts on wreck-sites develop some form of protective coating over their surfaces. This limits the availability of dissolved oxygen to the corroding surface and the rate of corrosion falls to a pseudo-steady state. In sea water this protective layer is normally calcareous in origin and in warm waters the growth of encrusting organisms can lead to iron artefacts being covered with a thick layer of encrustation after several centuries (North, 1976). Objects such as cannons and anchors exhibit characteristic voltages and acidities that are indicative of the rate of deterioration.

Following discussions during Dr Colin Martin's British Council-sponsored visit to Australia in 1993 it emerged that a corrosion study of iron objects on the Duart Point shipwreck (Martin, 1995) might add significant information about formation processes active on the site. Comparative data from a cold-water environment, moreover, would complement research into iron corrosion already undertaken by the writer on tropical and subtropical shipwrecks. With support from the British Council the site was visited between 25th and 30th July 1994, and a significant quantity of data obtained.

Experimental methods

Corrosion potential, or $E_{corr.}$, measurements are obtained by drilling through the marine growth and inserting a platinum electrode into the hole to establish electrical contact with the object. The reference electrode is placed adjacent to the point of measurement and the voltage, $E_{corr.}$, is read on a digital voltmeter in an underwater housing. Correct determination of the corrosion potential is normally indicated by the obtaining of a very steady voltage, that is, a reading that varies by only one or two millivolts over several minutes. Detailed discussions regarding the nature of $E_{corr.}$ are listed in other works (MacLeod, 1989a); the most important factor to note is that the rate of reduction of oxygen in the iron artefacts is directly related to the rate of reduction of oxygen dissolved in the sea water. This process is in turn related to the rate at which dissolved oxygen can diffuse to the corroding interface of the concreted object lying on the seabed. Thus the $E_{corr.}$ of a corroding artefact is seen to be very sensitive to a combination of temperature, salinity, and water movement.

Table 1. In situ *corrosion parameters for the Duart Point wreck (1653)*

Artefact	Corrosion depth mm	Average corrosion rate, mm yr	$E_{corr.}$* versus Ag/AgCl	pH
Cannon 1	61·5	0·164	− 0·452	5·42
Cannon 2	62·5	0·183	− 0·505	5·90
Cannon 3	64·5	0·189	− 0·503	5·63
Cannon 4	22·5	0·066	− 0·532	6·65
Cannon 5	6·5	0·019	− 0·512	6·85
Anchor	78·5	0·230	− 0·479	4·61

*The voltage of the Ag/AgCl reference electrode in sea water was +0·243 volts versus NHE, the standard hydrogen electrode.

The $E_{corr.}$ is the voltage of the corrosion cell that exists between oxidation of the iron and the reduction of the dissolved oxygen in oxygenated sea water. The voltage measured by a digital voltmeter refers to the difference in electrical potential of a silver chloride reference electrode (Ag/AgCl, sea water) and the platinum electrode in contact with the corroded metal. The encapsulated iron artefact will build up an acidic and chloride-rich microenvironment under the concretion layer (North, 1976). The acidity resulting from hydrolysis of metal ions and the increased concentration of chloride ions is due to inward diffusion from the surrounding sea water to achieve electrical neutrality of the corrosion products. By plotting the $E_{corr.}$ and the corresponding pH values for the artefacts on a Pourbaix diagram it is sometimes possible to determine the nature of the processes that are controlling the stability of objects in their particular micro-environments (Pourbaix, 1974).

In situ corrosion data

A series of dives on the Duart site enabled a set of corrosion potential and pH measurements to be determined on five of the seven cannons and the single anchor. A modified breast drill fitted with a 12·5 mm masonry bit was used to penetrate the concretion: an assistant located the bit and applied appropriate pressure via a steel cross-piece while the data-gatherer turned the handle. The latter periodically recorded the pH and the $E_{corr.}$ of the object as the drill bit probed the corroded matrix. The pH electrode had the same diameter as the drill bit. The electrode is fitted with a specially prepared flat glass bulb which is extremely sensitive and delicate—it is very easy to crack the glass and destroy the electrode. Once the drill bit encountered solid material, in the form of uncorroded metal, the depth of penetration was recorded. The depth of penetration, or graphitization, of cast iron is a very good indicator of the net effects of exposure to corrosive environments over time. The results of the measurements are summarised in Table 1. Previous work has established a direct relationship between the logarithm of the annual rate of corrosion of cast iron objects and the in situ corrosion potential (MacLeod, 1989b). A plot of data from the Duart Point wreck is shown in Fig. 1. By using the annual rates of corrosion, rather than the total amount of deterioration, comparison of data from other shipwrecks with different periods of immersion is facilitated.

The depths of corrosion on cannons 1, 2 and 3 are significantly higher than those recorded on cannons 4 and 5. The latter are also significantly lower than the average long-term corrosion rate of 0·1 mm yr recorded on a cannon recovered from the wreck of the Dartmouth (1690) in 1975, now in the conservation laboratories of the National Museums of Scotland, where the tests were carried out. The Dartmouth lies in 6 m of water some 4 km from the Duart Point wreck. The annual corrosion rate on cannons 1 to 3, as measured by depth of graphitization, is of the same order as that calculated for the second carronade from the wreck of HMS Sirius (1790) on Norfolk Island. The latter piece was located in 1·5 m of water in a depression in the reef platform, and had been subjected to continuous and dynamic surf action for two centuries. Its annual corrosion rate has been calculated at 0·196 mm yr.
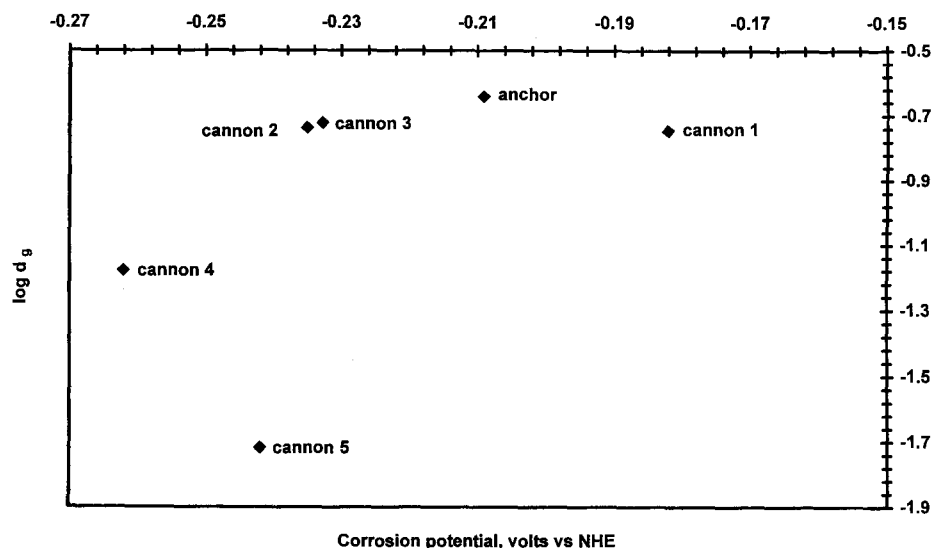
Figure 1. Plot of the log of the annual corrosion rate of iron artefacts and the *in situ* E_{corr}, volts versus NHE.

Clearly, cannons 1 to 3 at Duart Point, which show comparable corrosion rates, have been subject to major corrosive inputs during their 341 years of deposition. The strong ebb currents which sweep past the Point appear to be the major factor in the deterioration of metallic materials on this wreck-site, despite its average depth of 11·5 m.

During the investigation and measurement of the Duart samples it was noted that the concretion layer on cannons 1–3 was quite different from that on cannons 4 and 5. In contrast to the uniform whitish calcareous layer 1·5 mm thick on cannons 1–3, cannon 4 had a more dense, banded layer of concretion and black corrosion products, consistent with the object having fluctuated between exposure and burial (North, 1976). Because of its partial protection through periodic burial cannon 4 is much less corroded than cannons 1–3. The difference in microenvironment is even more pronounced in the case of cannon 5, which had suffered only a small degree of corrosion over its 341 years of immersion, with a graphitization depth of only 6·5 mm—a factor almost ten times smaller than that of cannon 3. The variability of corrosion extents on this site is clearly illustrated in Fig. 1. Inspection of the general site-plan (Martin, 1995, fig. 3) shows that cannons 1–3 are located close to the foot of the cliff, where the current

flow is particularly strong, and would therefore experience a more dynamic environment than cannon 4, which lies in a deeper and more open situation. Cannon 5, though in the dynamic zone, only partly protrudes from a seabed matrix from which, evidently, it has only recently emerged.

The corrosion potentials and corresponding pH data listed in Table 1 are plotted on a Pourbaix diagram at 11°C in Fig. 2. The choice of temperature for the diagram relates to the average seawater temperatures recorded during measurements on site. In the diagram the hatched area represents the region where ferrous ions, Fe^{2+}, are the thermodynamically favoured state of iron. All the artefacts are located in this region of stability which indicates that the metal is corroding freely in the absence of any protective oxide coating such as $Fe_2O_3.\chi H_2O$. The dominance of the ferrous ion also indicates that the microenvironment underneath the concretion is low in oxygen (reducing), whereas the seaward side of the concretion is associated with a strongly oxygenated environment.

There is a good correlation between the E_{corr} and the pH for cannons 2 and 3, and the anchor, since the points are seen to lie on a line where the E_{corr} falls by 0·0299 mV per pH. Oxidation of the parent metal to produce
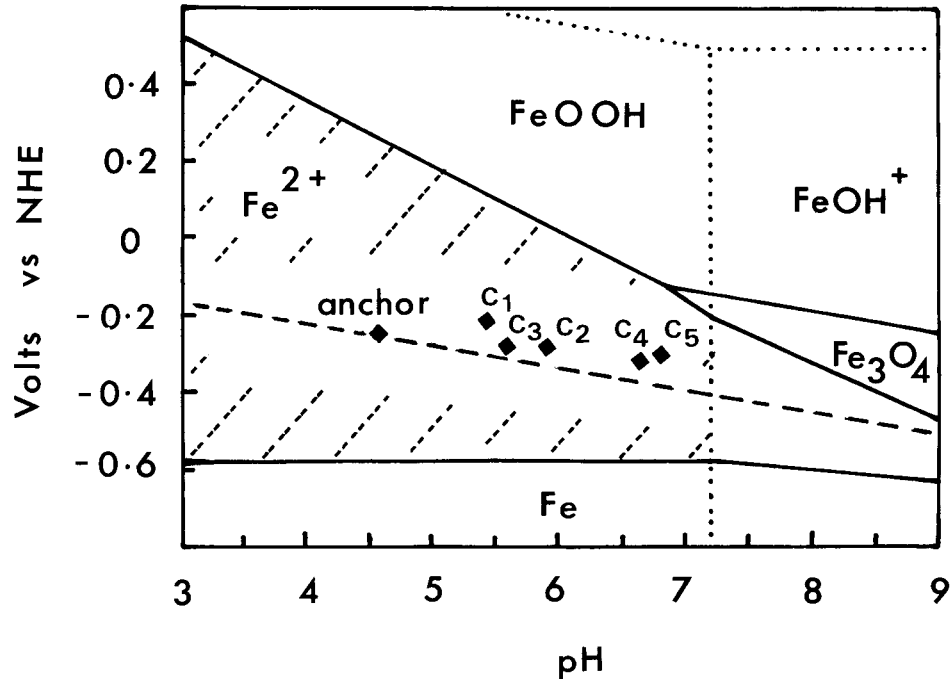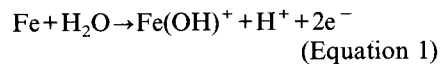
55

Figure 2. Pourbaix diagram for iron at 11°C and a dissolved ion concentration of $1 \cdot 0 \times 10^6$M, showing the *in situ* corrosion parameters for iron objects at Duart Point.

partially hydrolysed ferrous ions gives the same dependence as was observed empirically, thus the equation

$$Fe + H_2O \rightarrow Fe(OH)^+ + H^+ + 2e^-$$
(Equation 1)

would give the same dependence of $E_{corr.}$ on pH as was experimentally observed. Inspection of the Pourbaix diagram shown in Fig. 2 shows that the Duart Point data does not lie in the stability zone of the $FeOH^+$ ion and thus Equation 1 is not an accurate reflection of the process. Given that the corrosion is occurring in sea water, a more probable reaction scheme that incorporates chloride ions into the corrosion products is

$$2Fe + 2H_2O + 2Cl^- \rightarrow \{FeCl_2.Fe(OH)_2\} + 2H^+ + 4e^-.$$
(Equation 2)
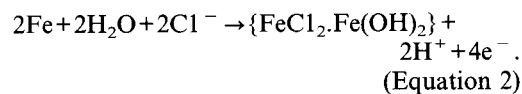
The partially hydrolysed ferrous chloride has been identified as a major intermediate reaction product in corrosion of marine iron (North, 1982). The above equation gives the same dependence of $E_{corr.}$ on the pH of the micro-

environment as was empirically observed. Thus a faster corrosion rate will produce greater acidity at the surface of the corroding metal underneath the marine growth. The same dependence of surface pH on $E_{corr.}$ that was noted for the Duart Point data was also observed with artefacts that were measured on the site of HMS *Sirius* on Norfolk Island (MacLeod, 1989b).

The anchor concretion was more dense than that on the cannons and was colonised by the pink coloured foraminifera. When the drill bit penetrated the concretion, copious amounts of gas were released. Previous studies of the gases released from corroded and concreted iron cannons and anchors have shown that the bubbles consist of a mixture of hydrogen, methane, nitrogen, and carbon dioxide (MacLeod, 1988). The $E_{corr.}$ and the pH of the anchor place it close to the limit of stability of water, with regard to its reduction to hydrogen. The calculated equilibrium partial pressure of hydrogen at the anchor voltage and pH is approximately 0·47 atmospheres. Laboratory tests in Edinburgh on a concreted cannon from

the *Dartmouth* showed that the gases, which evolved on penetration of the concretion, burned with the characteristics of a mixture of hydrogen and methane (Skinner, pers. comm., 1994).

The Duart Point anchor can only be described as having been extremely corroded, and is still undergoing active corrosion. Although chemical analyses of ordnance is normally reported on a weight percent basis, the electrochemistry of iron is controlled by the activity of the iron itself and this is directly related to its atomic composition. If we assume that the Duart Point iron artefacts have compositions typical of other 17th-century guns and anchors (Carpenter, 1993), the effective concentration of iron in the cast-iron cannon is of the order of 80 atom%. Since the wrought-iron anchor would have had a low carbon content, the iron is in an inherently more active form and close to 98 atom%. Given that no major differences exist between the overall physical chemical environments of cannon 3 and the anchor, it is possible that the cause of the 22% greater corrosion rate of the anchor is partly a reflection of the differences in composition between the two artefacts.

Discussion of results

Where the annual depth of corrosion is plotted as a function of the corrosion potential the data set of the anchor and cannons 1 and 2 has a multiple correlation coefficient of 0.9981 for the linear regression which gives the equation

$$\log d_g = 3.70 \, E_{corr.} + 0.228,$$
(Equation 3)

where d_g is the annual depth of corrosion in mm yr and the $E_{corr.}$ values have been corrected to the hydrogen scale (NHE). Similar linear relationships have been reported for iron artefacts on other sites but the 'slope' or dependence on $E_{corr.}$ and the intercepts were different (MacLeod, 1981; Carpenter, 1993). Although the marine concretion thickness of 1.5 mm on the cannon and anchor was much thinner than the 32 mm on the HMS *Sirius* carronade (MacLeod, 1994a), the Duart Point concretions were still able to sustain a significant pH profile between the surrounding seawater and the corroding metal surface. The surface pH for cannons 2 and 3 and the anchor showed a

linear dependence on the logarithm of the annual depth of corrosion

$$pH = -12.66 \log d_g - 3.47.$$
(Equation 4)

This correlation clearly indicates that the surface pH of the artefacts is directly related to the rate of deterioration of the materials, with the most acidic pH readings associated with the greatest rate of corrosion.

Having established the linear relationship between $E_{corr.}$ and $\log d_g$ in Equation 3 we can use it to calculate the present corrosion rate of the other cannons on the site by substituting their $E_{corr.}$ in Equation 3 and calculating the corrosion rate. The results of these calculations show that the current rates of corrosion are significantly higher than those indicated by the total depth of corrosion that has occurred over the past 341 years. The calculated rates indicate that cannon 1 has increased by 76%, cannon 4 by 123%, and cannon 5 by 810%. These results clearly indicate that the present *in situ* values of $E_{corr.}$ and pH are indicators that show the site has undergone major changes in recent times. The 80 mv less negative voltage of E_{corr} of cannon 1 compared with cannon 4 means that cannon 1 is now corroding twice as fast as cannon 4.

Implications for site management and conservation

As previously noted, the Duart Point data gives a steeper slope for the dependence of $\log d_g$ than the average recorded for several sites in Australia. It was recently reported that the data from the wreck of the *Lively* (c. 1812) had a significantly lower slope of 2.84 for Equation 3, but the significance of the difference was not apparent (MacLeod, 1989b). The *Lively* is located in the warm tropical waters of the Rowley Shoals some 400 km off the Western Australian coast. The data from Duart Point sheds new light on these relationships and makes the connection between the slope and the dissolved oxygen concentration in the sea water. The value of 3.70 for the slope in the cold (11°C) and less saline (34 ppt) waters of the Sound of Mull (Ellett, 1983) is greater than the 3.05 value for a series of sites in the warmer (22°C) and more saline (36 ppt) Australian waters. The concentration of dissolved oxygen

is interdependent on the salinity and the temperature, with the concentration going up with decreased temperatures and decreasing salinity (Riley & Skirrow, 1975: 561–2). By consulting the tables of dissolved oxygen concentrations it is possible to gain typical values for the three sites listed above. When the slope of Equation 3 is plotted as a function of oxygen concentration we find the following relationship

$$\Delta \log d_g / \Delta E_{corr.} = 10\cdot33 \log [O_2] - 4\cdot57,$$
(Equation 5)

where the concentration of oxygen is recorded in cm^3 dm^3. The implications of this relationship are of major significance in that once the salinity and temperature of the seawater, and hence the dissolved oxygen concentration, is known, Equation 5 can be used to calculate the relationship between corrosion rates and the $E_{corr.}$ values recorded for the artefacts on a site. In simple terms this means that it is now possible to determine the differences in the rates of corrosion for artefacts in similar chemical environments. At least one set of data on $\log d_g$ would be needed to determine the value of the constant in Equation 3 to allow a quantitative calculation of corrosion rates to be made.

One practical consequence of the relationship between the corrosion rate and the $E_{corr.}$, defined in Equation 3, and the way in which the slope of that relationship varies with the concentration of dissolved oxygen, is that maritime archaeologists now have a tool for monitoring changes in the conditions of the artefacts. Repeated visits to the SS *Xantho* site showed that the corrosion potential measurements on the boiler were reproducible within ± 2 mV over several seasons (MacLeod, 1992). If there are larger differences in corrosion potentials then it is possible to state that a change has occurred. The slopes of equation 3 for various sites are listed in Table 2, along with the corresponding Tafel slopes and the percentage change associated with a 3 mV shift in corrosion potential.

The Tafel slope is the number of millivolts that equates to a tenfold change in corrosion rates (Kiss, 1988). Because of the high concentration of dissolved oxygen at Duart Point it takes only 270 mV to bring about a tenfold increase in the corrosion rate. In the warm

Table 2. *Corrosion monitoring parameters for selected shipwreck sites*

Wreck-site	Slope v^{-1}	Tafel slope mV	% change
Duart Point	3·70	270	2·5
Average Australian	3·05	328	2·1
Lively (c. 1812)	2·34	427	1·6

tropical waters surrounding the *Lively* it requires 427 mV to bring about the same change in corrosion rates. It should therefore come as no surprise to see that a 3 mV shift in $E_{corr.}$ amounts to a larger percentage change in corrosion rate at Duart Point than on the *Lively* site. Laboratory experiments with a concreted diving knife that had been lost for ten years on the SS *Xantho* (sunk 1872) site has confirmed the same type of dependence of the Tafel slope on the dissolved oxygen concentration (MacLeod, 1994b).

Future management options

The *in situ* corrosion measurements at Duart Point indicate that several of the cannons are now corroding at a greatly increased rate, and that the remaining iron artefacts are probably corroding at a significant rate because of the high levels of water movement on the site. While archaeological information is preserved in the graphitized zone of the cast iron cannons, the original surface details on the anchor are in danger of becoming lost because of the low carbon content. Cannons 4 and 5 are not in imminent danger of collapse, so efforts need to be concentrated on preserving the anchor and cannons 1–3. It is important to consider what the best management options might be for this historically important site. Recent examples of exercising *in situ* treatment options were demonstrated on the wreck of HMS *Sirius*. This decision was reached after similar *in situ* studies had indicated a rapid rate of corrosion of a second carronade in the surf zone. After some three and a half years of pre-treatment with sacrificial anodes the extensively corroded carronade was raised in a largely stabilized condition (MacLeod, 1994a). After only eighteen months of laboratory treatment the carronade is nearing the end of its conservation

programme. The matching gun which received no pre-treatment took a total of nearly five years of conventional electrolytic reduction in the laboratory. Pre-treatment on the seabed of the bower anchor on HMS *Sirius* (MacLeod, 1987) has resulted in the preservation of the finest 18th-century anchor yet to be recovered and stabilized from an Australian shipwreck site.

During future seasons the remaining two cannons should have the pH and their $E_{corr.}$ measured so that appropriately informed decisions regarding their future can also be made. It would be wise to attach sacrificial anodes to cannons 1–3 and to the anchor to stop any further corrosion and to begin the conservation of these historically significant items *in situ*.

References
Carpenter, J. & MacLeod, I. D., 1993, Conservation of corroded iron cannon and the influence of degradation on treatment times. *ICOM Committee for Conservation, Preprints 10th Triennial Conference, Washington*, II: 759–766.

Ellett, D. J. & Edwards, A., 1983, Oceanography and inshore hydrography of the Inner Hebrides. *Proceedings of the Royal Society of Edinburgh*, **83B**: 143–160.

Kiss, L., 1988, Kinetics of electrochemical metal dissolution. *Studies in Physical and Theoretical Chemistry*, **47**: 60.

MacLeod, I. D., 1981, Shipwrecks and applied electrochemistry. *Journal of Electroanalytical Chemistry*, **118**: 291–303.

MacLeod, I. D., 1987, Conservation of corroded iron artefacts—new methods for on-site preservation and cryogenic deconcreting. *IJNA*, **16**: 49–56.

MacLeod, I. D., 1988, Conservation of corroded concreted iron. *Proceedings of Conference 28, Australian Corrosion Association*, I, 2–6: 1–9.

MacLeod, I. D., 1989a, The application of corrosion science to the management of maritime archaeological sites. *Bulletin of the Australian Institute of Maritime Archaeology*, **13.2**: 7–16.

MacLeod, I. D., 1989b, Electrochemistry and conservation of iron in sea water. *Chemistry in Australia*, **56.7**: 227–229.

MacLeod, I. D., 1992, Conservation management of iron steamships—the SS *Xantho* (1872). *Multi-disciplinary Engineering Transaction*, **GE No. 1**: 45–51.

MacLeod, I. D., 1994a, Conservation of a carronade from the wreck of HMS *Sirius*. *Newsletter ICOM—CC Metals Working Group*, **12**: 3–4.

MacLeod, I. D., 1994b, Unpublished observations.

Martin, C. J. M., 1995, The Cromwellian shipwreck off Duart Point, Mull: an interim report. *IJNA*, **24**: 15–32.

North, N. A., 1976, The formation of coral concentrations on marine iron. *IJNA*, **5**: 253–258.

North, N. A., 1982, Corrosion products on marine iron. *Studies in Conservation*, **27**: 75–83.

Pourbaix, M., 1974, *Atlas of Electrochemical Equilibria in Aqueous Solutions*. NACE, Houston (second edition).

Riley, J. P. & Skirrow, G., 1975, *Chemical Oceanography*, I (second edition). New York.

Skinner, T., 1994, Personal communication, Edinburgh, 9th August.